Asian Journal of Biomedical and Pharmaceutical Sciences
ISSN : 2249 - 622X

RESEARCH ARTICLE

Received on: 01-09-2013
Accepted on: 20-09-2013
Published on: 15-10-2013

G.S.Uthayakumar *
St.Joseph's College of Engineering, Chennai-119,Tamil Nadu,India.
Email:g_uthayakumar@hotmail.com,

QR Code for Mobile users

Conflict of Interest: None Declared !

Biomedical Optical spectroscopy techniques for Diagnosis of Human saliva sample

G.S.Uthayakumar[1],J.Chandhuru[2],S.Inbasekaran[3],A.Sivasubramanian[4]
[1,2]Department of Electronics and Communication Engineering,
[3]Department of Biotechnology,
[1, 2,3]St.Joseph's College of Engineering,Chennai-119,Tamil Nadu,India
[4,5,6]CSIR,Chennai-600025

Abstract

Fourier Transform Infrared Spectroscopy (FTIR) used for biomedical diagnosis of human saliva sample. Saliva is taken for experimental analysis from a normal person and also from a Gastric problem related patient. The spectral bio-diagnosis of normal human saliva sample shows the following vibrational functional groups O-H at 3305 cm^{-1}, C-H from 2928 to 2856 cm^{-1}, C=N and C=C obtained at 1658 cm^{-1}, C-H bend at 1455 cm^{-1}, C=S and C-C from 1159 to 1064 cm^{-1}, C-H out of plane bend at 748 cm^{-1} and 483 cm^{-1} assigned for C-H deformation.

Keywords- Absorption, Scattering, Transillumination, and Fourier transform infra-red spectroscopy, Fourier Transform-Raman spectroscopy.

Cite this article as:
G.S.Uthayakumar,J.Chandhuru,S.Inbasekaran,A.Sivasubramanian. Biomedical Optical spectroscopy techniques for Diagnosis of Human saliva sample. Asian Journal of Biomedical and Pharmaceutical Sciences 03 (24); 2013; 12-21.

1. INTRODUCTION

Fourier Transform Infrared Spectroscopy (FT-IR) and Fourier Transform Raman (FTR) spectroscopy analytical techniques are being used to identify the structural functional groups present in a human tissue sample [1-2]. Many research suggested an interesting method of assigning functional group frequencies observed in vibrational spectra. The FTIR have been thoroughly investigated and detailed vibrational band assignments have been made in this work. The assignment of the fundamental frequencies is made on the basis of magnitude and relative intensities of the absorption peaks. Vibrational energy and bond stretching frequency are determined by several molecular properties including atom types, atomic mass, molecular geometry, hydrogen bonding and bond order (single bond versus double bond versus triple bond). It is important to know that Raman scattering measures molecular polarisibilty (the extent to which an electronic cloud can be distorted), as molecular vibrations can affect polarisibilty providing useful information on molecular dipoles. Hence, intra-molecular and intermolecular vibrations are Raman active. Unlike Raman spectroscopy (symmetric vibrations) FTIR requires a dipole movement change (asymmetric vibrations). Accordingly, weak Raman scatters tend to be strong IR absorbers and include bond vibrations present in polar moieties such as carbonyl and hydrogen bonded hydroxyl groups, since they display asymmetric (FT-IR) rather than symmetric (Raman) vibrations. Several excellent reviews [3-5] discussed in detail the FT-IR and FT Raman effect. The various types of Raman spectroscopy, Raman band frequencies [6-8] and the many applications of FT-IR and FT Raman in chemistry, Biology, Material science and Medicine are shown in table 1. FT Raman spectroscopy can provide important information on molecular composition, structure, conformation, the degree of order and/ or disorder, phases and phase transitions, inter and intra-molecular interactions, hydrogen bonding, polymorphs, hydrates, anhydrates, molecular conformations and polymer conformations. The main objective of this research work is to identify the functional groups in the normal person saliva sample and compare it with a patient having gastric problems. We have identified number of functional groups present in the normal human saliva sample and found it to be more than those functional groups obtained from the saliva sample taken from gastric problem reported person after taking a drug sample (orange).

1.1 SALIVA AS A DIAGNOSTIC FLUID

Saliva is the body's mirror. The ability to use saliva to monitor the health and disease state of an individual has been considered as a highly desirable goal for health promotion and health care research. However, the growing appreciation of saliva as a mirror that can reflect virtually the entire spectrum of normal and disease states is relatively recent. Saliva can reflect tissue levels of natural substances and a large variety of molecules introduced for therapeutic, dependency, or recreational purposes; emotional status; hormonal status; immunological status; neurological effects; and nutritional and metabolic influences. A major drawback to using saliva as a diagnostic fluid is the fact that informative analytes (substances undergoing analysis) are generally present in lower amounts in saliva than in blood. However, with new and highly sensitive techniques, the lower level of analytes in saliva is no longer a limitation. Almost anything that can be measured in blood can be measured in saliva. Saliva has been reliably used to detect HIV 1 and 2 and viral hepatitis A, B, and C. It can also be used to monitor a variety of drugs including marijuana, cocaine, and alcohol.

Saliva is an effective diagnostic fluid to monitor health and diseases as it is inexpensive, non-invasive, and easy-to-use. As a clinical tool, saliva has many advantages over blood. Saliva is easy to collect, store, and ship, and it can be obtained at low cost and in sufficient quantities for analysis. For patients, the non-invasive collecting techniques dramatically reduce anxiety and discomfort and simplify the gathering of repeated samples for longitudinal monitoring over time. For professionals, saliva collection is safer than blood tests, which can expose health care providers to HIV or hepatitis virus. Saliva is also easier to handle for diagnostic procedures since it does not clot, lessening the manipulations required. Saliva-based diagnostics are therefore more accessible, accurate, less expensive, and present less risk to the clinician than current methodologies.

1.2 Gastric problems and Diagnosis

Food is one of the important consummate consumed by us to get energy. The food that we take is digested in the stomach by the action of gastric juice and Hydrochloric acid. Digested food is assimilated in the small intestine where the required carbohydrates, amino acids, fatty acids and water molecules are absorbed. The disturbance in the normal function of both stomach and intestine is responsible for gastric problems. There is no single cause for gastric problems. Peptic ulcers, irritable bowel syndrome, diverticulosis, inflammatory bowel disease, gastroesophageal reflux disease (GERD), gastritis and gastroenteritis are the major causes for gastric problems. Most of the ulcers are caused by infection with a bacterium called

Helibacter pylori or by use of pain medication like aspirin. Apart from microbial infections our food habits is also responsible for causing gastric problems. In few cases reported so far Gastric problems when untreated leads to gastric cancer. So there is a greater for diagnosing gastric problems. There are number symptoms through which we can confirm the onset of gastric problems like abdominal pain, vomiting, diarrhoea, dyspepsia, burning in chest, swallowing disorders and constipation. Though we find these many symptoms none of them is helpful in confirming the severe gastric disorders at their initial stages. Gastric disorders due to bacterial infection are confirmed only when the severity of the disease has reached to the culminant stage. These situations have triggered us to use optical devices like FTIR and FT- Raman instruments to identify Gastric problems at the earlier stage.

Types of Laser Scanning Raman	Analytical Application
Fourier Transform Raman Spectroscopy	Common method used in process, quality and quantity control applications in pharmaceutical systems
Raman micro-spectroscopy	Chemical imaging and mapping
UV resonance Raman Spectroscopy	Polypeptide and biopolymer secondary structure and conformational transitions
Surface Enhanced Raman Spectroscopy	Colloidal dispersions, Molecular self-assemblies, inclusion complexes, nanoparticles, surfaces and monolayers; chemical sensing biochemical analysis; rheology and gelation of hydrogels; interfacial molecular interactions
Resonance –enhanced Raman spectroscopy	Specific analysis of a material existing within a complex or a mixture of materials
Red-excitation dispersive Raman spectroscopy	Respirable pharmaceutical powders for pulmonary inhalation aerosol delivery
Linear Raman Spectroscopy	Aqueous aerosols

Table 1: Applications of Spectroscopy

2. Experimental Setup

All FTIR spectra presented and discussed in this research paper were collected on a research grade instrumental setup with both micro and macro sampling capabilities. The infrared spectrum originates from the vibrational motion of the molecule. The vibrational frequencies are a kind of the fingerprint of the compounds. This property is used for characterization of organic, inorganic and biological compounds. The band intensities are proportional to the concentration of the compound and hence qualitative estimations are possible. The IR spectroscopy is also carried out by using Fourier Transform technique. The interference pattern obtained from a two beam interferometer as the path difference between the two beams is altered, when Fourier transformed, gives rise to the spectrum. The transformation of the interferogram into spectrum is carried out mathematically with a dedicated on-line computer. Instrument details: Model: Spectrum one: FT-IR spectrometer, Scan range: MIR 450-4000 cm^{-1}, Resolution: 1.0 cm^{-1}, sample quantity used: 50mg, solid or liquid. The Perkin Elmer Spectrum 1 FT-IR instrument consists of globar and mercury vapour lamp as sources, an interferometer chamber comprising of KBr and mylar beam splitters followed by a sample chamber and detector. Entire region of 450-4000 cm^{-1} is covered by this instrument. The spectrometer works under purged conditions. Solid samples are dispersed in KBr or polyethylene pellets depending on the region of interest. This instrument has a typical resolution of 1.0 cm^{-1}. Signal averaging, signal enhancement, base line correction and other spectral manipulations are possible.

3. Materials and Methods

Orange sample was given to the patient suffering from gastric problems. Orange sampleconsistsofthefollowing composition Ispaghula Husk (Mentagoovata): 85.57%, Methylparaban: 0.2%, Propylparaban: 0.02%.Ispaghula seed husk has been used as a dietary fiber supplement to promote the regulation of large bowel function [9]. It is used in folk medicines as demulcent, emollient and laxative. In recent studies it has been shown to lower the blood cholesterol level[10].

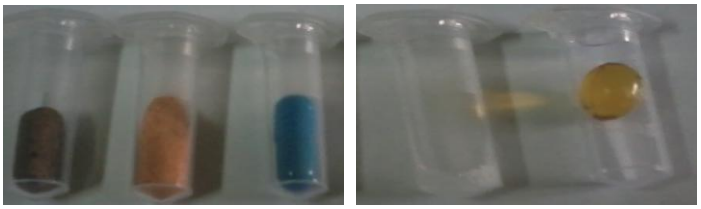

Figure 2 Samples taken for experiments

Ispaghula Husk Plant

Conventional methods used to confirm gastric problems

The stomach is located in the left upper part of the abdomen immediately below the diaphragm. The stomach is more or less concave on its right side, convex on its left. The concave border is called the lesser curvature, the convex border, the greater curvature. The region that connects the lower oesophagus with the upper part of the stomach is

called the cardia. The uppermost adjacent part is fundus. The fundus adapts to the varying volume of ingested food (or drug for disease in the body) and it frequently contains a gas bubble, especially after a meal. The largest part of the stomach is called as body. The lower most part of the stomach is the antrun, and it is usually funnel-shaped, with its narrow end connecting with the pyloric region. The latter empties into the duodenum. The upper division of the small intestine.Biological tissues in the gastro intestine tract express mechanical properties in between the solid and fluid properties i.e., the deformation is finite, the stress-strain relation is nonlinear , there is a pronounced visco elastic component and anisotropy prevails due to the heterogeneous laminated structure. Due to the high water content in biological tissues, they express mechanical properties of both an elastic solid and viscous fluid. The longitudinal, radial and circumferential directions are symbolized by z , r and Θ. The pressure (P) from a bolus or a distending balloon induces a normal stress that will stretch the tube in circumferential directions and radial compression (a thinner wall). Longitudinal extension may also occur. A moving bolus will also cause shear stresses in the mucosa.

The stomach function as

- An expansile reservoir that allows the rapid consumption of large meals , the process is facilitated by receptive relaxation of the proximal stomach in response to food and is called gastric accommodation,
- A digestive and absorptive organ that breaks down large protein and carbohydrate molecules and thus facilitates their absorption in the stomach and the small intestine,
- A part of the endocrine and immune system, it secretes hormones and neurotransmitters, e.g. Gastrin, fristamine, endorphin, somatostatin , serotonin and intrinsic factor and
- A biomechanical system that grinds mixes, forms and periodically discharges the performed chyme into the duodenum as the physical and chemical condition of the mixture is rendered suitable for the next phase of digestion

The biomechanical properties are time dependent, in that the stress-strain response does not occur instantly. When the drug is suddenly strained and the strain is maintained constant, the corresponding stresses induced in the wall decrease with time. This phenomenon is called stress relaxation. If the drug is suddenly stressed and the stress is maintained constant, the drug will continue to deform. This phenomenon is called creep. If the loading process is different from that in the unloading process, then the drug is subjected to a cyclic loading. This phenomenon is called hysteresis. The effectiveness and diversity of physiological responses of the stomach to internal and external stimuli depend on the inherent activity of fristo morphological elements, namely, smooth muscle cells, neurons and interstitial cells of cajal, and their topographical organization in gastric tissue. In the gastro intestinal tract, we must consider the external forces from the environment. The GI tract is a part of forces from the environment and the forces it generates by itself. When external forces (from outside or from the lumen) are applied to a GI segment, it deforms, resisting the forces. It is common practice to use distensibility and stiffness to describe the deformation and the resistance to deformation respectively.

STRESS

Consider a large and a small specimen. The large specimen can sustain a large force whereas a small specimen can sustain a much smaller force. Stress is force per unit cross-sectional area. On any surface, the force may be applied perpendicular to the surface, such as the bolus pressure (normal stress) exerted on the wall, or parallel to the surface, such as the force exerted by the fluid flow (shear stress) ion the wall. Normal stresses may be either compressive or tensile. A force may be applied in any direction and can induce stresses and strains in various directions. At any given point in the body, the state of stress is described by a stress tensor that consists of the three normal stresses and six shear stresses, three of which are independent.

These nine component of stresses (τ_{ij}, j =1, 2, 3) are sufficient for fully specifying the state of stress at the point P (Figure 1). This means that stress is a second order tensor. Similar considerations can be made for strain, i.e. strain also consists of nine components. Since both stress and strain are second order tensor qualities, the stress-strain relation will be of the fourth order i.e. will contain 81 components. Thus, in general, it would require 81 elastic constants to characteristic a drug taken by a patient fully .Assumptions such as the isotropy assumption can reduce the number of components considerably. For e.g. if the stress and strain tensors are symmetric, the number of constants are reduced to 36. Here $\tau_{11,}$ $\tau_{22,}$ τ_{33} are the normal stresses and the remaining six components are shear stresses. In this paper, we assume that the GI tract is a thin walled cylindrical pressure vessel and that the weight of the pressure vessel and its contents can be neglected (argument for studying the tissue when it is immersed in a fluid-filled organ bath)

CIRCUMFERENTIAL STRESS:

During luminal pressure loading, the equilibrium condition requires that the force in the intestinal wall in the circumferential direction be balanced by the

force in the intestinal lumen contributed by the inflation pressure. When the geometry is cylindrical, the average circumferential wall stress is,

$$\tau_\theta = P_{ri}/h \quad \ldots\ldots\ldots\ldots\ldots\ldots\ldots\ldots \quad (1)$$

Where P is the pressure, r_i is the internal radius, h is the wall thickness.

Consider a cylindrical intestine subjected to an internal pressure P_i as shown in Figure 3a. The pressure in the intestine induces stress in the intestinal wall. Under equilibrium conditions, the force in the intestinal wall in the circumferential direction $2\tau_\theta (r_o - r_i)$ L, is balanced by the force in the intestinal lumen contributed by the pressure $2Lr_iPi$ as shown in Figure 3.3 C. Hence under equilibrium conditions, $2\tau\theta$ (ro – ri)L = 2LriPi and the circumferential stress.

$$\tau_\theta = P_{ri}/(ro-ri) \quad \ldots\ldots\ldots\ldots\ldots\ldots\ldots\ldots \quad (2)$$

Comparing equation (1) and (2)

h = (ro – ri)

The effectiveness and diversity of physiological responses of the stomach to internal and external stimuli depend on the inherent activity of histomorphological elements, namely smooth muscle cells, neurons and interstitial cells of cajal, and their topographical organization in gastric tissue. Smooth muscle cells are embedded into a network of collagenous and elastin fibres and are coupled via gap junctions into three distinct syncytia (muscle layers). The external longitudinal muscle layer continues from the oesophagus into the duodenum. The middle uniform circular layer is the strongest and completely covers the stomach. The circular fibres are best developed in the antrum and pylorus. At the pyloric end, the circular muscle layer greatly thickness to form the pyloric sphincter. The innermost oblique muscular layer is limited chiefly to the cardiac region.

Elastin and collagen fibers are structural proteins built into a 3-D supporting network. Elastin may be structured to 250% of the unloaded configuration. While collagen is relatively inextensible reinforced protein, and the main load carrying element. Collagen fibres are undulated in the undeformed state and become stiff when straightened under the action of external applied loads. The overall state of soft tissues is strongly correlated with their content. The uttermost tunica serosa is formed of densely packed collagen and elastin fibers that coat the entire organ and thus provide its final shape.The submucous coat and mucous membrane of the stomach consist of loose epithelial and glandular cells. Their main function is digestion and immune response. Their role in the biodynamics of the organ, i.e. force stretch ratio development, propulsion etc. is negligible.Motor propulsive activity in the stomach originates in the upper part of the body of the organ. Three types of mechanical waves are observed. The first two types are small isolated contraction waves and peristalic waves that slowly move from the point of origin down towards the pyloric sphincter. These three types of contraction produce slight or deep indentations in the wall and serve as mixing, crushing and pumping mechanism for the gastric contents. The third type of wave is non-propagating in nature and is a result of the tonic simultaneous contraction of all muscle layers that are normally superimposed on small and peristalic contraction.After the transplantation of any organ in the human body is hyposalivation is possible after 100 days, it may be indicative for a graft versus host disease. In these situations sodium and lysozyme concentrations are increased, while phosphate and s-IgA are decreased in saliva.

DIABETES MELLITUS:

Due to decrease in salivary flow rate, patients with diabetes mellitus express higher levels of amylase and secretory IgA in whole saliva constituents.

ALCOHOLIC LIVER CIRRHOSIS:

Patients with alcoholic liver cirrhosis,50% reduction in the salivary flow rate and a reduction of salivary sodium, bicarbonate and chlorine concentration. The total salivary protein concentration decreases as well.

EPILEPSY:

Patients with epilepsy who take phenytoin due to increasing of collagen synthesis and accumulation of proteoglycans, gingival hypertrophy can be observed. These patients should have a high quality oral hygiene. IgA deficiency is another side effect of phenytoin, resulting in a decreased immunological defense.

BURNING MOUTH SYNDROME:

Dry mouth can be developed after taking some medications like antidepressant. Their salivation can be easily increased mechanically and chemically. The total salivary protein concentration of stimulated saliva is lower than in control subjects, but the total mucin concentration is higher salivary potassium, chloride and phosphate concentration are also increased in these patients.

KIDNEY DYSFUNCTION:

50% of all hemodialysis patients complain of hyposalivation changes in taste, ammonium smelling breath and oral mucosal pain. These tests are invasive, expensive and sometimes conclusive. Researches are measured specific concentration of cytokines in saliva of patients with Sjogren'ssyndrome. Lactoferrin , Beta-2 microglobulin, Lysozyme C, cystatin C, cystatin S, sodium, chloride, Albumin, Alpha 2 microglobulin, Lipid and inflammation mediators such as Eicosanoids, Prostaglandin E2, Thrombosome B2 and Interleukins 2 and 6. IgA, IgG and IgM auto antibodies arised in individuals that suffer from auto immune diseases. Levels of amylase, carbonic anhydrase and phosphate

decrease in saliva but levels of calcium and potassium are usually normal. SS. Antila antibodies in saliva can be useful in diagnosis of Sjogren's syndrome as well as in control of its progression. Parotid saliva from patients with rheumatoid arthritis and Sjogren's syndrome contains higher level of multiple forms of tissue kallikrein.

CELIAC DISEASE:

Due to mal absorption of gluten, celiac disease is created in the small intestine. The detection of IgA and antigliadin antibody in saliva shows high specificity and low sensitivity, their determination in serum is highly sensitive and less specific.

CYSTIC FIBROSIS (CF):

There are several electrolyte and protein concentration differences and increased visco-elasticity of saliva in cystic fibrosis patients, compared with healthy individuals. The RNase activity is four times higher in CF homozygotes than in control subjects. The salivary concentrations of sodium, phosphate, chloride, lipid, EGF and prostaglandin E2 play an important role in protection against dental cavity.

GRAFT-VERSUS-HOST DISEASE:

As destruction of the salivary gland tissues, there is decrease in salivary flow rate, the graft- versus-host disease is created.

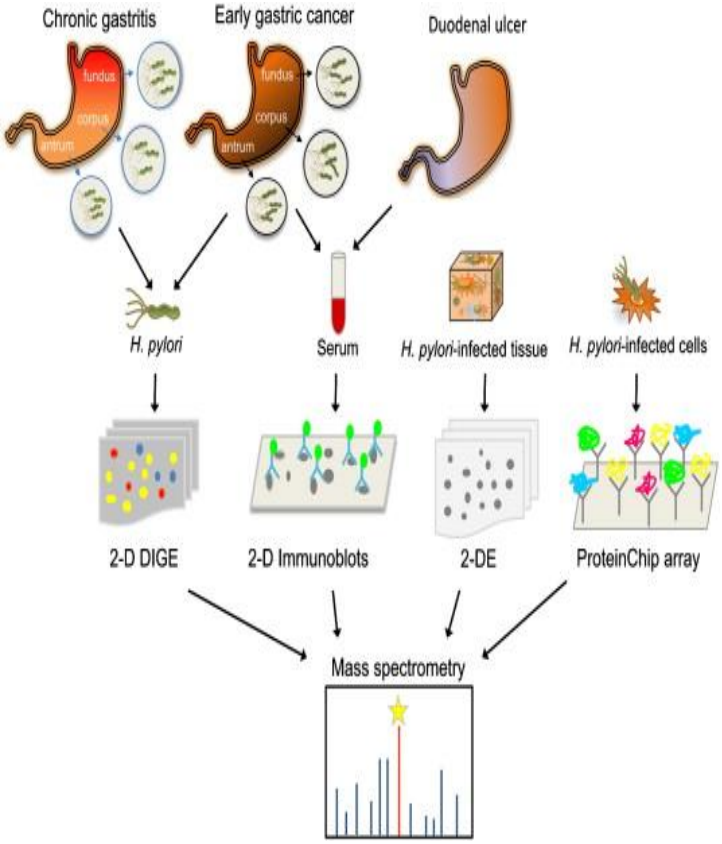

Method to confirm the gastric Problems

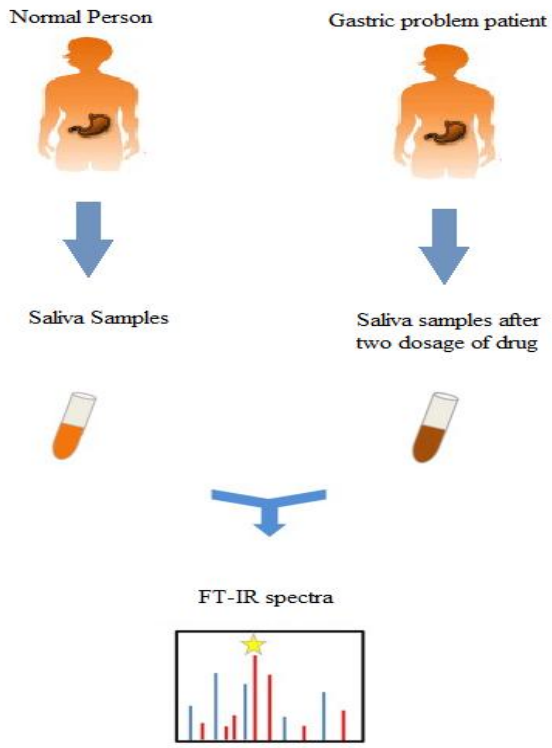

4. Mathematical modelling of Photon transport

Mathematical modelling of photon transport is based on Maxwell's equations of electro dynamics relating the electric and magnetic field intensities E and H to the electromagnetic inductions D and B, respectively.

Maxwell's equations in differential form

$$\nabla x E = \frac{-\partial B}{\partial t}$$

$$\nabla x H = \frac{\partial D}{\partial t} + J_f$$

$$\nabla \cdot D = \rho_f$$

$$\nabla \cdot B = 0$$

Where ρ_f is the density of all free electric charges and J_f is the density of all electric currents of the photons.

The laser beam itself is approximated by a plane EM-waves

$$E(r,t) = E_o \exp(i(wt - kr))$$

$$H(r,t) = H_o \exp(i(wt - kr))$$

Where 'k' is the propagation vector of the EM-wave. Assuming the relative magnetic permeability of the tissue to be μ = 1, the EM inductions can be expressed as

$B = \mu_o H$

$D = \varepsilon\varepsilon_o E$

Where μ_o and ε_o are the EM constants, and ε is the dielectric factor of the photon. The first two equations leads to $K \times E = \omega \mu_o H$

$K \times H = -\omega\varepsilon\varepsilon_o E + iJ_f = -\omega\varepsilon\varepsilon_o E + i\sigma E$

Where σ is the electric conductivity of the photon. Hence,

$K \times (K \times E) = -\omega^2\varepsilon\mu_o\varepsilon_o E + i\omega\mu_o\sigma E$

$$K \times (K \times E) = -\left(\frac{\varpi^2}{C^2}\varepsilon + i\frac{\varpi\sigma}{\varepsilon^2\varepsilon_o}\right)E$$

Where $C = \sqrt{\frac{1}{\mu_o\varepsilon_o}}$ is the speed of the light.

Electromagnetic waves are transversal, i.e., kE = 0, the amount $k = |k|$ can be expressed by

$$K^2 = \frac{\varpi^2}{C^2}\varepsilon_i$$

With the complex dielectric factor

$$\varepsilon^i = \varepsilon - i\frac{\sigma}{\omega\varepsilon_o}$$

In the case of negligible absorption, $k = \frac{\omega}{c}n$

Where 'n' is the index of refraction. Since the tissue absorbs incident radiation, then

$$K = \frac{\omega}{c}(n + i\alpha)$$

Where α is the index of absorption. Combining leads to the general expression

$$\varepsilon^i = (n + i\alpha)^2$$

The following two relations are derived

$$n = \frac{c}{\omega}\mathrm{Re}(k)$$

$$\alpha = \frac{c}{\omega}\mathrm{Im}(k)$$

The tissue absorption co-efficient

$$\alpha_{at} = -2\,\mathrm{Im}(k) = -\frac{2\omega}{c}\alpha_{at}$$

Therefore,

$$\mathrm{Re}(\varepsilon^i) = n^2 - \alpha_{at}^2$$

$$\mathrm{Im}(\varepsilon^i) = 2n\alpha_{at}$$

$$\alpha_{at} = \frac{1}{2n}\mathrm{Im}(\varepsilon^i)$$

Stating that the existence of an imaginary part of z' evokes absorption.

The equation of motion of a tissue electron,

$$m_e\frac{\partial v_e}{\partial t} = -eE - v_{ei}m_e v_e$$

Where m_e is the electron mass, v_e is the electron velocity, e is the electron charge, v_{ei} is the mean collision rate of free electrons and ions. Assuming that the tissue electrons are performing oscillations induced by the incident electromagnetic field at its frequency w, we obtain

$$iwm_e v_e = -\varepsilon E - v_{ei}m_e v_e$$

$$v_e = -\frac{eE}{m_e(v_{ei} + i\omega)}$$

Therefore,

$$J_f = -N_e v_e$$

Where N is the density of free electrons

$$J_f = \frac{Ne^2 E}{m_e(v_{ei} + iw)}$$

Therefore

Substitute the conductivity value,

$$\varepsilon^i = \varepsilon - i\frac{1}{\varepsilon_o\omega}\cdot\frac{Ne^2}{m_e(v_{ei} + iw)} = \varepsilon - i\frac{\omega^2}{\omega(v_{ei} + iw)}$$

$$\varepsilon^i = \varepsilon - \frac{w^2 w_{at}^2}{w^2 v_{ei}^2 + w^2} - i\frac{wv_{ei}\cdot w_{at}^2}{w^2 v_{ei}^2 + w^2}$$

Where w_{at} is the tissue frequency defined by

$$w_{at}^2 = \frac{Ne^2}{\varepsilon_o m_o}$$

The tissue absorption co-efficient is derived as

$$\alpha_{at} = \frac{w}{nc}\cdot\frac{wv_{ei}w_{at}^2}{w^2 v_{ei}^2 + w^2} = \frac{v_{ei}}{nc}\cdot\frac{w_{at}^2}{w^2 + v_{ei}^2}$$

Therefore, tissue absorption is enhanced in the IR region of the spectrum, since $w_{at} \sim N$ and $v_{ei} \sim N$,

Therefore, $\alpha_{at} \sim N^2$

Stating that the absorption is a nonlinear function of the free electron density and thus,of the absorbed energy itself.

5. Results and Discussions

In the FTIR spectra, the C=C asymmetric stretching vibrations occur in the region of 2037cm^{-1}. As solids or liquids, primary aliphatic amines absorb in the region 3434cm^{-1} – 3450cm^{-1}, and exhibit a broad band of medium intensity. In a dilute solution in non-polar solvents, two bands are observed for primary amines due to N-H asymmetric and symmetric vibrations in the range 3550cm^{-1} – 3250cm^{-1}. The relative intensity of

the bands due to the hydroxyl stretching decreases with an increase in the concentration with additional broader bands appearing at lower frequencies 3580cm^{-1} – 3200cm^{-1}.In aminobenzoesaesure the hydroxyl stretching occurs at 3434cm^{-1} in the FTIR spectra. From the above band assignments, the sample under experiment shows a very strong band at 3434cm^{-1} in the FTIR spectrum due to N-H and O-H stretching.The carbonyl groups exhibit a strong absorption band due to C=O (saturated aldehyde) vibration at 1728cm^{-1}(Figure 1).

From Figure 2 the following observations were obtained for the orange sample using FT-Raman spectroscopy. The wave numbers 1728.19cm^{-1} to 2235.36cm^{-1} was assigned to the C=C functional group with strong intensity. The wave numbers 900.21 to 984.86cm^{-1} was assigned to the CC alicyclic and aliphatic chain with medium intensity. The wave number 2554.97cm^{-1} to 2665.88cm^{-1} was assigned to the S-H functional group with strong intensity. The wave number 4952.37 cm^{-1} and 3205.69cm^{-1} was assigned to the O-H functional group. The functional group CH_2 & CH_3 asymmetry was obtained at the wave number 1466.24cm^{-1}.The functional group C-H was obtained from 2758.98cm^{-1} to 2921.10cm^{-1} with strong intensity value. The methyl group was obtained at 1353.20cm^{-1} and 1099.99cm^{-1} was assigned to C=S with strong intensity value. The wave number 3290.44cm^{-1} was assigned to N-H functional group with weak intensity.

5.1 Saliva of human body

In previous research works, Fourier Transform Raman Spectroscopy was used to investigate the molecular changes of structural proteins in human skin subjected to strain. In the Raman spectrum of unstrained skin, bands assigned mainly to collagen and elastin were observed at 1658 cm^{-1} (amide I), 1271 and 1255 cm^{-1} (amide III), and 935 and 817 cm^{-1} (C-C stretching modes of the protein backbone). Moreover, bands characteristic for amino acids were observed at 1336 cm^{-1} (desmosine), 1004 cm^{-1} (phenylalanine), 919 and 856 cm^{-1} (proline), and 877 cm^{-1} (hydroxyproline). Positions and intensities of the listed Raman bands were analyzed as a function of applied strain(Table.1).

Wave number (cm^{-1})	Wavelength λ (nm)	Frequency GHz	Photon energy	Functional group	Intensity
3917	2552.97	117510	778621.26	-	-
3899	2564.76	116970	775043.22	-	-
3884	2574.66	116520	772061.52	-	-
3867	2585.98	116010	768682.26	-	-
3766	2655.34	112980	748605.48	-	-
3725	2684.56	111750	740455.5	-	-
3305	3025.72	99150	656967.9	O-H	W
2928	3415.30	87840	582027.84	CH_3 and CH_2C-H stretch	S
2856	3501.40	85680	567715.68	CH_3 and CH_2C-H stretch	S
2305	4338.39	69150	458187.9	-	-
1658	6031.36	49740	329577.24	C=N, C=C	S
1542	6485.08	46260	306518.76	-	-
1455	6872.85	43650	289224.9	C-H bend	M
1159	8628.13	34770	230386.02	C=S, C-C	S
1064	9398.49	31920	211501.92	C=S, C-C	S
748	13368.98	22440	148687.44	C-H out of plane bend	S-M
483	20703.93	14490	96010.74	C-H deformation	S

Table.1 Wavenumber assignment of Saliva sample with functional group

C =N stretching vibrations

These bands occur in the region 1610-1680 cm^{-1}. The absorption band at 1658 cm^{-1} observed in the FTIR analysis corresponds to C=N stretching vibrations.

O-H vibrations

The existence of bands in the region 3550-3200 cm^{-1} is due to inter molecular hydrogen bonding existing between the solute and solvent molecules. In the present case the band at 3305 cm^{-1} is assigned to O-H stretching vibrations(Figure.3 a,b).

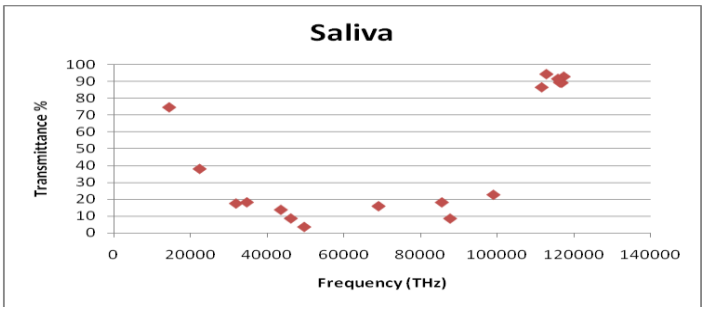

a.Frequency verus Transmittance

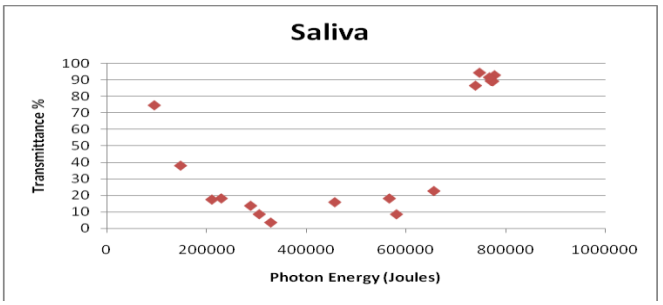

b. Photon energy verus Transmittance

Figure.1 Human body fluid(Saliva sample)

C-C stretching vibrations

These bands can be observed in the region 600-1300 cm^{-1}. In the present case the bands in the region 1159 and 1064 cm^{-1} is assigned to C-C stretch in the aliphatic chain.

C-H vibrations

The C-H stretching vibration bands occur in the region 2900-3100 cm^{-1}. The C-H bend vibration bands occur in the region 1300-1500 cm^{-1}. The bands in the region 2928 and 2856 m^{-1} in the FTIR analysis is assigned to methyl and methylene C-H bond asymmetric and symmetric stretching vibrations. The band in the region 1455 cm^{-1} is assigned to methylene C-H bond bending and methyl C-H bond asymmetric bending. The band in the region 748 cm^{-1} is assigned to C-H bond out of plane bend and the peak at 483 cm^{-1} i\corresponds to C-H deformation.

C=S stretching vibrations

These bands occur in the region 1000-1250 cm^{-1}. In the present case absorption band at 1159 and 1064 cm^{-1} is assigned to C=S stretching vibrations.

C=C stretching vibrations

The C=C stretching vibrations occur in the region 1620-1680 cm^{-1}. In the present case the band at 1658 cm^{-1} is assigned to alkenyl C=C stretching vibrations.

5.2 Interpretation of human body Saliva with drug

O-H vibrations

The existence of bands in the region 3550-3200 cm^{-1} is due to inter molecular hydrogen bonding existing between the solute and solvent molecules. In the present case the band at 3306 cm^{-1} is assigned to O-H stretching vibrations(Table.2).

C-N vibrations

Medium to weak absorption bands for the unconjugated C-N linkage in primary, secondary and tertiary aliphatic amines appear region of 1250-1020 cm^{-1}. In the present case the FTIR bands observed at 1061 cm^{-1} is assigned to C-N stretching vibrations of primary amine.

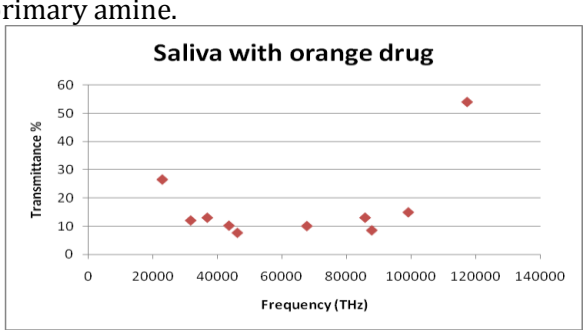

a.Frequency Vs Transmittance

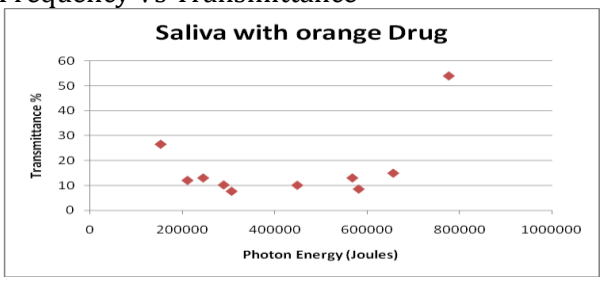

b. Photon energy Vs Transmittance

Figure.2. Saliva with Drug sample

C≡C vibrations

The C≡C stretching vibrations occur in the region 2100-2300 cm^{-1}. In the present case band in the region 2259 cm^{-1} is assigned to C≡C stretching vibrations.

Wavenumber (cm^{-1})	Wavelength (nm)	Frequency (THz)	Photon Energy	Functional group	Intensity
3912	2556.24	117	777627.36	-	-
3306	3024.80	99	657166.68	O-H	S
2929	3414.13	87	582226.62	CH_3 and CH_2 C-H stretch	S
2860	3496.50	85	568510.8	CH_3 and CH_2 C-H stretch	S
2259	4426.74	67	449044.02	C≡C	M
1542	6485.08	46	306518.76	-	-
1456	6868.13	43	289423.68	C-H bend	S
1232	8116.88	36	244896.96	C-N	M
1061	9425.07	31	210905.58	C-N	M
768	13020.83	23	152663.04	C-H out plane bend	S-M

Table.1 Wavenumber assignment of Saliva sample after taking drug

C-H vibrations

The C-H stretching vibration bands occur in the region 2900-3100 cm^{-1}. The C-H bend vibration bands occur in the region 1300-1500 cm^{-1}. The aromatic C-H out of plane bend bending vibrations occurs in the region 900-667 cm^{-1}. In the present case absorption band at 2929 and 2860 cm^{-1} is assigned to methyl and methylene C-H asymmetric or symmetric stretching vibrations. The absorption band at 1456 cm^{-1} is assigned to methylene C-H bend and methyl C-H asymmetric and symmetric bending. The absorption band at 768 cm^{-1} is assigned to C-H out of plane bending vibrations(Figure.4 a,b,c.).

Conclusion

It can be clearly seen from the FTIR spectrum of the human saliva sample that the functional groups present in the patient having gastric problem after taking two dosage of drug's almost similar to the normal person's saliva. From this we can affirmatively say that FTIR can be used to diagnose gastric problem. It can also be used to find whether complete cure has been attained after the medication period. The following chemical elements are found in the human body fluid samples. The vibrational band assignments of the drugs are summarized in the table 1 and table 2 and are discussed as follows.

(i)**Ring Vibration**

The bands exhibited in the region around 3000cm^{-1} can be immediately assigned to be due to aromatic C-H stretching's . In this view, the vibrational frequencies exhibited at 3434 cm^{-1} in the FTIR Spectrum are considered to be due to C-H stretching vibrations occur in the region 1642-1579 cm^{-1} in FTIR Spectra.

(ii)**N-H/OH Vibrations**

As solids or liquids, Primary aliphatic amines absorb in the region 3434 cm^{-1}- 3450 cm^{-1} and exhibit a broad band of medium intensity. In dilute solution in non-polar solvents, two bands are observed for primary amines due to N-H asymmetric and symmetric vibration in the range 3550 – 3250 cm^{-1}.The relative intensity of the band due to the hydroxyl stretching decreases with the increase in concentration with additional to broader bands appearing at lower frequencies 3580 - 3200 cm^{-1}. In aminobenzoesaesure the hydroxyl stretching occurs at 3434 cm^{-1} in FTIR. From the above band assignments. The Sample under experiment shows a very strong band at 3434 cm^{-1} in FTIR spectrum due to N-H and O-H stretching vibrations.

(iii)**Deformation vibrations**

A number of C-H in plane deformation bands occur in the region 973-901 cm^{-1}, the bands being sharp but week to medium intensity. However, these bounds are not normally of importance for interpretation purpose although they can be used. The aromatic C-H out of plane deformation bands occurs below 700 cm^{-1}. The bending vibrations are generally found at lower wave numbers. The frequencies observed at 775, 705, 576, 592 to 491 cm^{-1} are assigned to be due to O=C-C, O=C-N, C=C-N and C=C-C bendings of the pyrimidine ring in the FTIR Spectra of Xanthine and C-N-C bending vibrations are assigned at 498 and 428 cm^{-1} . Using the above analogy, the bends at 901cm^{-1} – 775 cm^{-1} is due to C-H in plane deformation. The bands at 676 $cm^{-1}$is due to C-H out of plane deformation/C-C=O deformation.

References

1. Uthayakumar GS and Sivasubramanian A, "Biomedical optical spectroscopic techniques to characterize the medicinal drug Fibril-SF", International journal of Biomedical Engineering and Advanced research" Vol.4 (No.1), pp 16-23,Jan.2013.

2. Uthayakumar GS and Sivasubramanian A, "Monitoring of Drugs at molecular level using FTIR spectroscopy" Journal of Biotechnology Biomaterials", 2012,2:6 http://dx.doi.org/10.4172/2155-952X.S1.016

3. Uthayakumar GS, Sivasubramanian A "Fiber Optic Transillumination Imaging System and Human Body Relations". Open Access Scientific reports, Vol.1 Issue.7, 2012, 1:376. doi:10.4172/scientificreports,376

4. Uthayakumar GS, Sivasubramanian A "Characterization and Quantization of Medicinal Drugs using Biomedical Optical Spectroscopy Methods" International journal of Engineering Research and Technology" ISSN 2278-0181,Vol.2, Issue.2, Feb.2013

5. Uthayakumar GS, Sivasubramanian A "Characterization of Medical Drugs Using Biomedical Optical Techniques", International Journal of Biomedical Engineering and Consumer Health Informatics (IJBECHI), ISSN: 0973-6727 (Vol.4 No.2 2012). Pages: 43-50.

6.Uthayakumar GS, Sivasubramanian A "Monitoring of Human body tissues at Molecular Level using FOTI Systems"8th International symposium on Bioinformatics Research and applications, May 21-23,2012, University of Texas at Dallas,Dallas,Texas,Pages.133-147.

7. Uthayakumar GS, Seetharaman.R ,Kumaravel.N, "Mobile phone Antenna and its radiation pattern" Transactions of the IRE Professional (2008)

8.Al-Rawhani, Mohammed A. Design and Implementation of a Wireless Capsule Suitable for Autofluorescence Intensity Detection in Biological Tissues , IEEE Transactions on Biomedical Engineering, Vol(60) , Issue: 1 **,** pp: 55 – 62, Jan. 2013

9.Denkçeken, T. , Simsek, T.; Erdogan, G.; Pestereli, E.; Karaveli, Şeyda; Ozel, D.; Bilge, Uğur; Canpolat, Murat ,Elastic Light Single-Scattering Spectroscopy for the Detection of Cervical Precancerous Ex vivo, IEEE Transactions on Biomedical Engineering, Vol(60**)** , Issue: 1 , pp: 123 – 127, Jan. 2013

10. Nguyen, Hien M. , Peng, Xi; Do, Minh N.; Liang, Zhi-Pei Denoising MR Spectroscopic Imaging Data With Low-Rank Approximations, IEEE Transactions on Biomedical Engineering, Vol(60) , Issue:1,pp: 78 – 89, Jan. 2013.

11. Pashaie, R., Falk, R. Single Optical Fiber Probe for Fluorescence Detection and Optogenetic Stimulation, IEEE Transactions on Biomedical Engineering, Vol**(**60),Issue: 2 ,pp: 268 - 280 , Jan. 2013.